A Model-in-the-Loop Interface to Emulate Source Dynamics in a Zonal DC Distribution System

Weidong Zhu, Steve Pekarek, *Member, IEEE*, Juri Jatskevich, *Member, IEEE*, Oleg Wasynczuk, *Senior Member, IEEE*, and Dana Delisle

***Abstract*—A model-in-the-loop capability (MIL) has been developed to emulate the dynamics of alternative power sources in a hardware-based dc zonal electrical distribution system. Using this tool, models of the power sources are simulated in real-time and interfaced with hardware components at the voltage and current levels of the power system. Coupling between simulation and hardware is established through a dc/dc power converter using model/wall-clock time synchronization. The MIL capability is illustrated in the emulation of a synchronous machine/converter power source. Results of time-domain and frequency-domain studies are provided to validate the approach.**

***Index Terms*—DC distribution testbed, dynamics, hardware-in-the-loop, real-time simulation, stability.**

I. Introduction

HARDWARE-IN-THE-LOOP (HIL) is a valuable tool for designing complex interconnected systems. Within HIL, the data acquisition subsystem, communication network, and/or computational hardware/software that are to be used to implement the control algorithms are first interconnected with a computer model of the system to be controlled. Initial evaluation of the controller is then performed using a computer model to emulate system performance. The advantages of using HIL as a design step (as opposed to starting with actual hardware) include reduced cost, availability of the system, and the ability to test operating states (damaged, faulted, etc) that may not be permitted with hardware. The uses of HIL technologies to analyze and design the monitoring and control subsystems of interconnected power systems are well documented [1]–[5]. In [1] an HIL system is designed to test the controls for an electrical locomotive propulsion system. In [2], a real-time model of a three-phase ideal-source rectifier is interfaced with a controller that is used to establish thryistor gate signals. In [3], the dynamics of a vehicle are modeled in real-time to test the controls for an antilock brake actuation system. In [4], a simulation environment that can be used for HIL testing of power electronic components is described. In [5], controllers are evaluated using a real-time model of a STATCOM. Although the applications vary, a commonality of HIL approaches is that the interface between the model(s) and the hardware is at a low voltage and power level commensurate with the inputs and outputs of the control system. In this way, the monitoring and control hardware/software can be readily evaluated and, if necessary, fine-tuned or debugged before interconnection with the actual power system.

Recently, there has been impetus to extend HIL concepts to interconnect computer models of selected components/subsystems, such as individual motor drives or generators, with the actual power system at the higher voltage and power levels commensurate with the power system [6]–[8]. Specifically, in [6] the dynamics of an inverter/induction machine is studied using a hardware-based inverter and a real-time simulation of an induction machine. To couple the model of the induction machine with the inverter, the stator currents obtained from the induction machine model are used as commanded currents to an ac/ac converter that is coupled to the inverter. In [7], a utility power system is modeled using a combination of real-time digital models of components and hardware components. The interaction of digital models of components and hardware of power system components is achieved using high-power amplifiers. Details of the amplifier circuits are not provided in [7]. In [8], the researchers suggest possible approaches to partition hardware/software components for ac radial distribution systems. As described in [6]–[8], an HIL in which models and hardware are interconnected at the voltage/power levels of the power system [herein referred to as model-in-the-loop (MIL)] capability enables system integrators to identify potential source/load interactions and, if necessary, address these issues through computer modeling, thereby reducing risk and overall implementation costs.

An obstacle to a MIL interface is the scaling of the inputs and outputs of the computer model(s) to the voltage and power levels commensurate with the actual system. A second important issue is establishing time-domain models of components that can be executed in real-time. Each of these issues is addressed in this paper. In particular, an effective partitioning between the physical system and time-domain computer models is established for the power-electronic-based dc zonal electric distribution (dc ZED) testbed system shown in Fig. 1. This configuration is similar to that being considered for future naval power system architectures [9]. All of the testbed components, which include multiple power electronic converters, are realized in hardware and implemented at the University of Missouri-Rolla.

Manuscript received February 11, 2004; revised September 15, 2004. This work was presented at the IEEE Power Electronics Specialist Conference (PESC'03), Acapulco, Mexico, June 15-19, 2003. Recommended by Associate Editor B. Lehman.

W. Zhu is with the Department of Electrical Engineering, University of Missouri-Rolla, Rolla, MO 65409 USA (e-mail: pekarek@ece.umr.edu).

S. Pekarek was with the Department of Electrical Engineering, University of Missouri-Rolla, Rolla, MO 65409 USA and is now with Purdue University, West Lafayette, IN 47907 USA (e-mail: spekarek@purdue.edu).

J. Jatskevich is with the Department of Electrical Engineering, University of British Columbia, Vancouver, BC V6T 1Z4, Canada.

O. Wasynczuk is with the Department of Electrical Engineering, Purdue University West Lafayette, IN 47907 USA.

D. Delisle is with the Electrical System Division, Naval Sea Systems Command, Washington, dc 20376 USA.

Digital Object Identifier 10.1109/TPEL.2004.842973

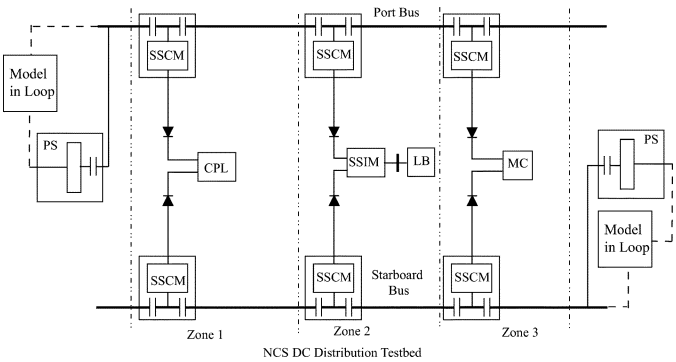

Fig. 1. Hardware-based dc distribution testbed.

Fig. 2. Hardware of the dc distribution testbed.

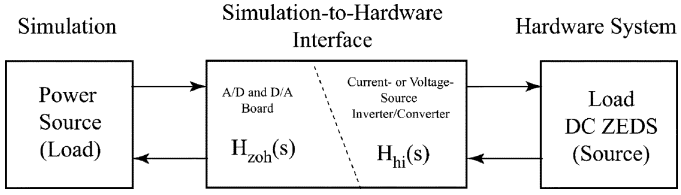

Fig. 3. Block diagram of a model/hardware interface.

To demonstrate the MIL interface set forth in this paper, the dynamics of the synchronous generator/rectifier sources are modeled in real-time using a commercial simulation program. An interface between the power system and the simulation of the generator/rectifier source is established using a dc/dc converter and customized model/wall clock time synchronization. Real-time execution of the computer model is achieved using a voltage-behind-reactance model of the generator/rectifier and judicious choice of integration method and its parameters.

The validity of the approach is established through using a series of time-domain and frequency-domain studies. The proposed approach utilizes a standard personal computer (PC) and operating system, and is readily adapted to models implemented across distributed computing platforms. Due to its low cost and relative simplicity, the proposed MIL interface provides additional flexibility and greatly reduces the capital required to analyze and design large-scale power-electronic-based systems.

II. Description of Study System

Although ac power distribution systems are commonly used in U.S. Navy ships and many submarines, with advances in power electronic devices, research is focusing on the implementation of dc ZED architectures versus conventional ac radial or zonal distribution systems. Specific interest in the design of dc ZED systems includes stability and dynamic performance under pulsed loads, power quality, efficiency, and survivability. In order to investigate these design issues, a dc distribution testbed has been constructed at the University of Missouri-Rolla based upon the topology shown in Figs. 1–2. The dc ZEDS considered consists of three zones, wherein power supplies (PS) are used to provide power to two main dc buses, namely Port and Starboard. Inside each zone, the power is regulated through converter ship service converter modules (SSCM) that share loads through a droop control. Zone 1 supplies a generic high-bandwidth converter-based constant-power-load (CPL) to emulate nonlinear dynamics of typical loads in power-electronic systems. In Zone 2, a ship service inverter module (SSIM) converts the dc to three-phase ac which supplies the load block (LB). Finally, Zone 3 contains a motor controller (MC) that is used to regulate torque and speed of an induction machine. The details of each component, including circuit diagrams and control parameters are fully documented in [9].

III. Model-in-the-Loop Interface

A block diagram depicting a general case of the MIL paradigm is shown in Fig. 3. Without loss of generality, in Fig. 3 the load is assumed to be realized in hardware and the power source is emulated using the real-time simulation. A conventional HIL system includes an interface between simulation and intermediate hardware at the voltage/power levels of the control interface. The simulation-to-hardware interface is realized using commercially available A/D and D/A boards that can be used with off-the-shelf PCs and readily interfaced with low-power level hardware. Assuming a finite sampling rate, this stage is depicted in Fig. 3 using a zero-order-hold (ZOH) transfer function $H_{zoh}(s)$.

In the MIL considered, an additional interface between the model/hardware is created at the voltage/power levels of the hardware system. Since the simulation output will be either a current or voltage, the intermediate hardware must be a current- or voltage-source converter, respectively, capable of providing the required current or voltage to the target hardware system (load). The converter response is determined by the respective control applied and the switching frequency. To prevent the overlap of converter dynamics with those of the component modeled in real-time, the switching period of the converter should be at least an order of magnitude smaller than the fastest time-constant of the component model. The converter transfer function is depicted in Fig. 3 as $H_{hi}(s)$.

In order to ensure that the MIL with hardware portrays the same dynamic properties as the actual all-hardware system, the combined effect of $H_{zoh}(s)$ and $H_{hi}(s)$ must be negligible in the frequency range of interest (assuming sufficient accuracy of the simulated models). In the example described herein, a wound-rotor synchronous generator connected to a rectifier is considered to represent the power source to the port and starboard busses. The components of the MIL system are illustrated

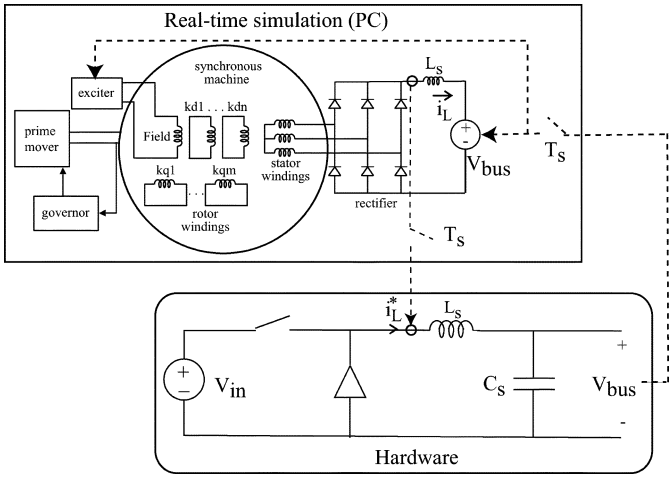

Fig. 4. Simulation-to-hardware interface.

in Fig. 4. As shown, the dynamics of a generator with its governor, prime mover, excitation system, and rectifier are simulated on a PC. The simulated rectifier inductor current represents an output of the real-time simulation and is used as a commanded current to the dc/dc (buck) converter. The buck converter regulates the port (starboard) bus voltage of the hardware testbed system. Power to the buck converter is supplied from an independent commercial dc power supply. The bus voltage is fed back into the simulation to represent the expected load on the synchronous generator and also as an input to an excitation control system.

The MIL components in this system include a 2-GHz Pentium-4 PC, a buck converter, an interface board and cable. The PC runs under the Windows XP operating system that provides the platform for all software. A commercial D/A board with 1.25 MS/S, 12-b resolution, and 16 analog inputs is used as the interface between the simulation output and the hardware. A hysteresis modulation scheme has been implemented for the switch-level control of the buck converter. The model is simulated with Matlab/Simulink [10] using the modeling tool described in [11] and the interface between real-time simulation and hardware is accomplished using the toolbox described in [12]. To describe a typical execution sequence, the time-domain simulation is advanced (integrated) one step at a time. Provided the CPU time required to solve the model is less than the numerical time step, the output of the simulation model is sent to the input of the D/A board and is used as the current command to the buck converter. The output of the voltage sensor on the port (starboard) bus is measured using a Tektronix P5200 high voltage differential voltage probe. The output of the probe is sent to the A/D input board used for simulation/hardware interface. The real-time toolbox contains a library of blocks with real-time input and output support. All features are implemented as blocks using a standard graphical interface of Simulink. A timer on the system board of the computer is used as the time base of the hardware system.

IV. Model-in-the-Loop Performance

As shown in Fig. 4, at synchronized intervals of time, both the inductor command current and the bus voltage are sampled and exchanged between simulation and converter hardware, respectively. The sampled inductor current represents the commanded current to the buck converter. If a hysteresis method is used to control switching of the converter, the time constant relating the commanded current to measured current (assuming a small-signal disturbance) is on the order of a switching cycle [13]. Therefore, in order to estimate the effect of errors resulting from the MIL interface, it is assumed that the combined effect of $H_{zoh}(s)$ and $H_{hi}(s)$ can be approximated as a zero-order hold [14]

$$G_{mil}(s) = \frac{1 - e^{-Ts}}{s} \tag{1}$$

where $T = 2\pi/\omega_{mil}$ is the sampling period of the A/D plus one switching period of the converter, and s is the Laplace operator. As shown in [13], under hysteresis control, current tracking is typically achieved in less than a switching cycle. Therefore, (1) represents a worst-case conservative estimate of the effect of the MIL interface. Substituting $j\omega$ for s and rearranging, (1) can be expressed as

$$G_{mil}(\omega) = \frac{2\pi}{\omega_{mil}} \frac{\sin\left(\frac{\omega\pi}{\omega_{mil}}\right)}{\left(\frac{\omega\pi}{\omega_{mil}}\right)} e^{-j\pi(\omega/\omega_{mil})}. \tag{2}$$

From (2), it is seen that the transfer function is essentially a low-pass-filter. Error is decreased as the ratio of ω/ω_{mil} decreases. At a ratio of 1/10, the amplitude of a signal at the base frequency is 98.4% of the actual. A phase difference of 18 degrees is introduced. In general, the sampling and switching frequencies must be sufficiently higher than the highest frequency of interest. In practice, the sampling rate is much more difficult to increase, since it is determined by the execution speed of the time-domain simulation. Judicious choice of the model structure and numerical algorithms are critical in achieving fast simulation and thus maximizing the sampling frequency.

V. Generator/Rectifier Model

Although real-time execution of models of electric machines connected to ideal sources has been documented [6], machine/converter component models are often computationally intensive and therefore difficult to simulate in real-time. Specifically, these systems tend to have a wide range of time constants, e.g., rotor dynamics may have time-constants at the order of seconds, while switching dynamics may have time-constants in micro-seconds. Further, for power electronic-based systems, analytically establishing a model for each switching topology can be a tedious, if not intractable task. To overcome this difficulty, it is common to utilize algorithmic methods to establish a state-model or a resistive-companion model of the system. Commercial packages that implement algorithms to solve circuits include EMTP, Spice, Saber, Matlab Power System Toolbox, etc. Regardless of the choice of package, there is overhead involved in the algorithmic process and therefore model structure is critical to minimize computational effort. Traditionally, the majority of representations of electric machine used in system simulations are based upon a reference frame transformation. Although reference frame transformations are extremely useful, it is often difficult to represent power electronic circuits in terms of transformed stator

variables. Therefore, in order to model a machine/electronic interface, a coupling between the transformed stator variables and the physical variables of the power electronic circuit must be developed.

In order to achieve real-time simulation of the generator/rectifier a so-called detailed physical-variable voltage-behind-reactance (DPVVBR) machine model [15] was found to be computationally very efficient and well suited for MIL. In the DPVVBR model, the stator voltage equations are expressed as

$$\mathbf{v}_{abcs} = \mathbf{r}_s \mathbf{i}_{abcs} + p[\mathbf{L}''_{abcs}(\theta_\mathbf{r})\mathbf{i}_{abcs}] + \mathbf{v}''_{abcs}. \tag{3}$$

In (3), $\mathbf{r}_s$ is a diagonal matrix consisting of stator winding resistances, and $\mathbf{L}''_{abcs}(\theta_r)$ is a matrix of the form

$$\mathbf{L}''_{abcs}(\theta_\mathbf{r}) = \begin{bmatrix} L''_s(2\theta_r) & L''_m\left(2\theta_r - \frac{2\pi}{3}\right) & L''_m\left(2\theta_r + \frac{2\pi}{3}\right) \\ L''_m\left(2\theta_r - \frac{2\pi}{3}\right) & L''_s\left(2\theta_r - \frac{4\pi}{3}\right) & L''_m(2\theta_r) \\ L''_m\left(2\theta_r + \frac{2\pi}{3}\right) & L''_m(2\theta_r) & L''_s\left(2\theta_r + \frac{4\pi}{3}\right) \end{bmatrix}. \tag{4}$$

The inductances $L''_s(2\theta_r)$ and $L''_m(2\theta_r)$ are functions of the subtransient inductances of the machine and the rotor position. Specifically

$$L''_s(\bullet) = L_{ls} + L''_a - L''_b \cos(\bullet) \tag{5}$$

$$L''_m(\bullet) = -\frac{L''_a}{2} - L''_b \cos(\bullet) \tag{6}$$

where

$$L''_a = \frac{(L''_{mq} + L''_{md})}{3} \tag{7}$$

$$L''_b = \frac{(L''_{md} - L''_{mq})}{3}. \tag{8}$$

In (7) and (8), L''_{mq} and L''_{md} are so-called q- and d- axis subtransient inductances.

The back-emf $\mathbf{v}''_{abcs}$ represents the coupling of the rotor and stator electromagnetic systems, which can be expressed in a form

$$\mathbf{v}''_{abcs} = [\mathbf{K}^r_s(\theta_r)]^{-1} \begin{bmatrix} v''_q \\ v''_d \\ 0 \end{bmatrix} \tag{9}$$

where

$$v''_q = \omega_r \lambda''_d + \sum_{j=1}^{M} \frac{L''_{mq} r_{kqj}}{L^2_{lkqj}} \left(\lambda''_q - \lambda_{kqj} + L''_{mq} i^r_{qs}\right) \tag{10}$$

$$v''_d = -\omega_r \lambda''_q + \sum_{j=1}^{N} \frac{L''_{md} r_{kdj}}{L^2_{lkdj}} \left(\lambda''_d - \lambda_{kdj} + L''_{md} i^r_{ds}\right) + \frac{L''_{md} r_{fd}}{L^2_{lfd}} (\lambda''_d - \lambda_{fd}) + \frac{L''^2_{md} r_{fd}}{L^2_{lfd}} i^r_{ds} + \frac{L''_{md}}{L_{lfd}} v_{fd} \tag{11}$$

and

$$\lambda''_q = L''_{mq} \sum_{j=1}^{M} \frac{\lambda_{kqj}}{L_{lkqj}} \tag{12}$$

$$\lambda''_d = L''_{md} \left(\frac{\lambda_{fd}}{L_{lfd}} + \sum_{j=1}^{N} \left(\frac{\lambda_{kdj}}{L_{lkdj}} \right) \right). \tag{13}$$

In (10)–(13), λ_{kqj} and λ_{kdj} represent the flux linkages of rotor damper windings and λ_{fd} represents the flux linkages of field winding. It is noted that there is a slight difference in the form of the DPVVBR model utilized herein and the one described in [15]. Specifically, herein the stator back-emf (10) and (11) contain terms that include rotor resistances multiplied by stator currents expressed in the rotor frame of reference (i^r_{qs} and i^r_{ds}). In [15], this term is not included in the back-emf, but rather is added to the stator resistance, to establish equivalent q- and d-axis stator resistances. When transformed to physical variables, these equivalent resistances appear as coupled stator resistances. Specifically, the stator resistance matrix of the DPVVBR model is nondiagonal. The two models are in fact identical. However, it has been found that some commercial simulation packages do not provide a means to include a nondiagonal stator resistance matrix. The dynamics of the rotor electrical and mechanical systems are expressed in state-model form as

$$p\lambda_j = -\frac{r_j}{L_{lj}} (\lambda_j - \lambda_{md}) + v_j, j = fd,\ kd1 \ldots kdN \tag{14}$$

$$p\lambda_j = -\frac{r_j}{L_{lj}} (\lambda_j - \lambda_{mq}),\ j = kq1, \ldots kqM \tag{15}$$

$$p\omega_r = \frac{P}{2J} (T_e - T_l) \tag{16}$$

$$p\theta_r = \omega_r \tag{17}$$

where T_e is the electromechanical torque produced by the generator, T_l is the load or traction torque applied on the shaft, and. ω_r and θ_r represent the electrical speed and position of the rotor.

A circuit/block diagram of the DPVVBR model is given in Fig. 5. As shown, when implementing the DPVVBR model, only the stator branches and nodes are included when defining the circuit topology. The rotor voltage equations are expressed explicitly in state model form with rotor flux linkages as state variables. The subtransient voltages represent outputs of the rotor model and are incorporated in the stator circuit as dependent sources. The stator branch currents are transformed into the rotor reference frame and represent inputs to the rotor state model.

The advantages of structuring the machine model in the form of (3)–(17) are numerous. First, models of machines can be directly coupled to complex networks that include switching converters without the need to establish an interface between network components represented in terms of physical-variables (i.e., power converters) and those that are represented in terms of transformed variables (traditional qd machine models). Second, the electrical and mechanical dynamics of the rotor are represented directly in state-model form. Since the dynamics of the stator windings of the machines and the network to which they are connected are generally orders of magnitude faster than those of the rotor electrical and mechanical subsystems, the partitioning provides a natural decoupling of time-scales. This is advantageous when utilizing stiff ODE solvers and/or multirate integration techniques [16]. Specifically, when utilizing stiff ODE solvers, the time-step can be increased as the stator transients subside. If multi-rate integration algorithms are applied, the partitioning allows one to partition and solve the respective fast and slow subsystems using different time steps (and possibly even distinct integration algorithms). In addition, if dynamic saliency is neglected, the inductances in (4) become independent of rotor position. If one utilizes a numerical algorithm to

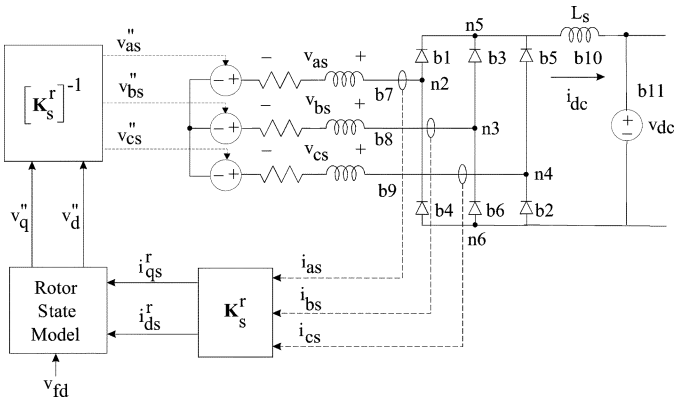

Fig. 5. Voltage-behind-reactance implementation.

TABLE I
PARAMETERS OF SYNCHRONOUS MACHINE

r_s = 382 mΩ	L_{ls}=1.12 mH	L_{mq}=24.9 mH	L_{md}=39.3 mH
r_{d1}=140 Ω	L_{ld1}=9.87 mH	r_{q1}=5.07 mH	L_{lq1}=4.21 mH
r_{d2}=1.19 kΩ	L_{ld2}=4.91 mH	r_{q2}=1.06 Ω	L_{lq2}=3.5 mH
r_{d3}=1.58 Ω	L_{ld3}=4.52 mH	r_{q3}=447 mΩ	L_{lq3}=16.2 mH
r_{fd}=112 mΩ	L_{lfd}=1.53 mH	N_s/N_{fd}=0.0269	P=4

generate a system model, such as the state model generation algorithm presented in [11], the elimination of rotor-position-dependent inductances allows one to generate the state model only at changes in system topologies. In contrast, if the state-model contains time-dependent terms, the state model must be updated at each numerical time step. Therefore, elimination of time-varying inductances can yield substantial computational savings when modeling synchronous machines. This may be particularly important when one is attempting to model components faster than real-time.

Utilizing the DPVVBR synchronous machine model, the stator-rectifier network is simulated using an automated state model generator program implemented as a toolbox for Simulink. The rotor state model and the rest of the power source subsystem are implemented in the same model using standard Simulink library blocks.

VI. RESULTS

In order to demonstrate the proposed MIL interface and hardware configuration, the power source composed of a synchronous machine/rectifier system described in previous section was implemented. The generator parameters, which correspond to a 3.7 kW synchronous machine in the UMR laboratory, are shown in Table I. The dc-link inductance L_s in Fig. 4 is 1.027 mH. In each of the studies, the machine/converter response was calculated using Heun's algorithm [17] with a fixed time step of 92 μs. The maximum sampling frequency for model/hardware interaction was 3.6 kHz. Both time-domain and frequency-domain studies were performed. A hysteresis modulated switching scheme was used to regulate the current of the buck converter.

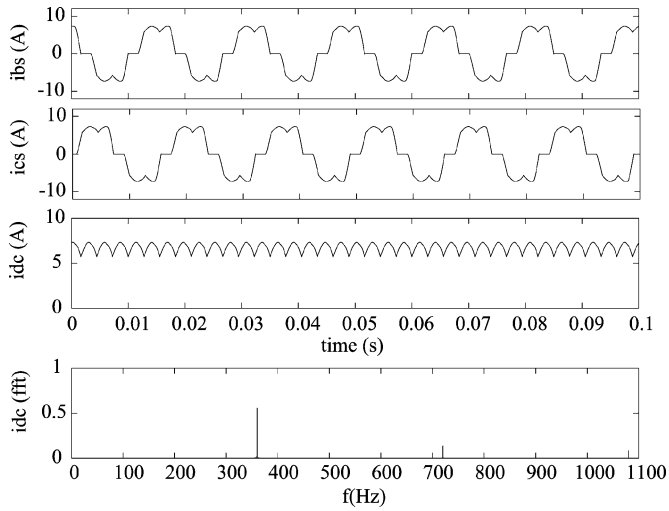

Fig. 6. Simulated steady-state response of machine/rectifier.

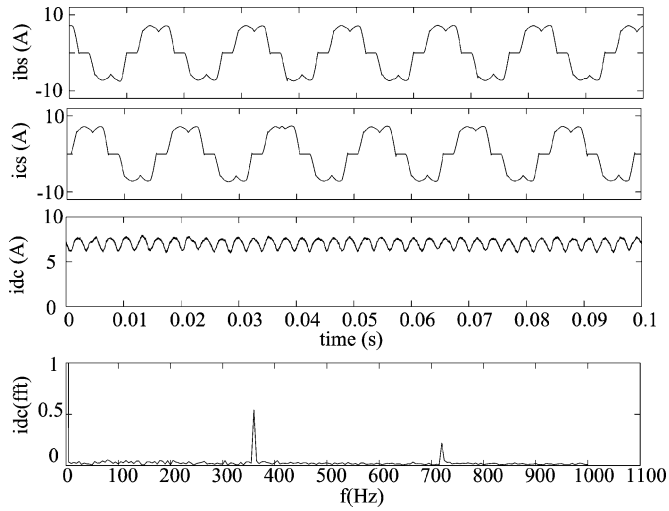

Fig. 7. Hardware with MIL steady-state response of machine/rectifier.

In the first study the port bus was connected to a single 27.7 Ω resistance. The response of the simulated machine/rectifier system with the respective load is provided in Fig. 6, wherein the phase-b and phase-c stator currents i_{bs} and i_{cs}, the dc inductor current i_{dc} and its frequency spectrum are shown. The response of the hardware system with the MIL power source, and identical load is shown in Fig. 7. To effectively compare simulated and measured responses, the switching frequency of the buck-converter was filtered from the measured response using a digital fast-average filter. Comparing Figs. 6 and 7 it is seen that the response of the hardware system with MIL is in very good agreement with that of the simulated machine/rectifier. The slight differences in the waveforms of the dc current are results from errors introduced by the ZOH sampling. Specifically, for a sampling frequency of 3.6 kHz, the error in the fundamental component of the dc current (360 Hz), is relatively minor (2.7%). However, at higher frequencies (720 Hz and above) the error increases ($> 60\%$).

To verify the dynamic performance, a step change in load was also performed. The dc/dc converter used to test the MIL strategy had a current rating of 15 A. To provide margin of safety

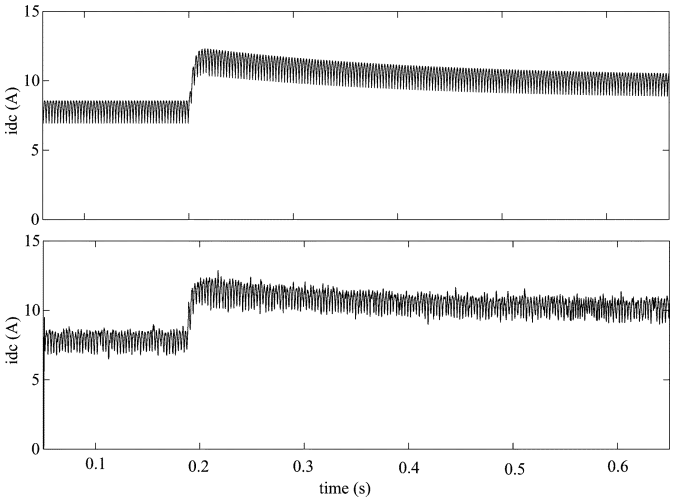

Fig. 8. Transient responses to the step-change in load.

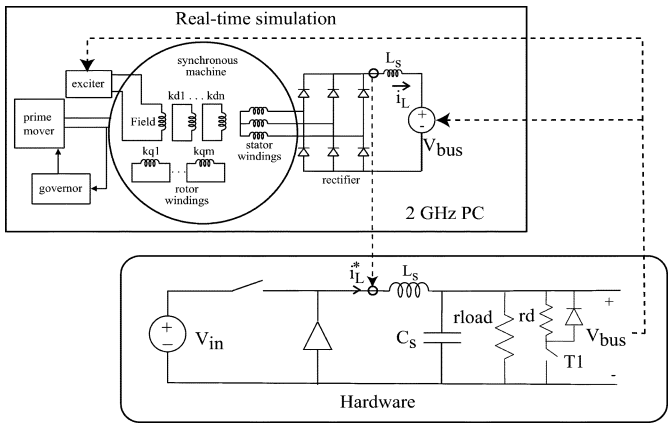

Fig. 9. Configuration used to measure impedance.

for testing transient conditions, a 20.5-Ω resistor was used to establish an initial steady-state operating current of approximately 8 A. This represented approximately 50% rated load for the generator. To introduce a transient, a second resistance was placed in parallel to provide a combined load resistance of 10 Ω. The field voltage was held fixed during the operation. The dc-link currents of the simulated machine/rectifier and hardware system with MIL are shown in Fig. 8. Comparing waveforms, it is seen that the transient response is well predicted.

For stability analysis, the output impedance of a power source is often of interest. For the hardware system with MIL, source output impedance was measured using the pulsating load method as shown in Fig. 9 and described in [18]. The resulting impedance looking into the power source from the dc-link capacitor is shown in Fig. 10, wherein it is also compared against the impedance predicted by the detailed simulation (switching of rectifier represented). As can be seen, both magnitude and phase match very well particularly in the low frequency range. As the disturbance frequency approaches within a decade of the rectifier switching frequency (360 Hz), a difference in the measured and simulated impedance is seen. This is expected, since as the small-signal disturbance frequency approaches the switching frequency, their interaction makes it difficult to characterize the impedance exactly.

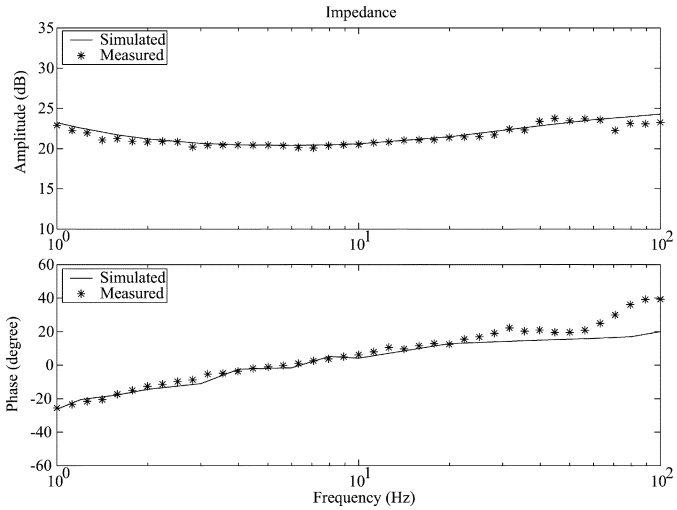

Fig. 10. Measured and simulated source impedance.

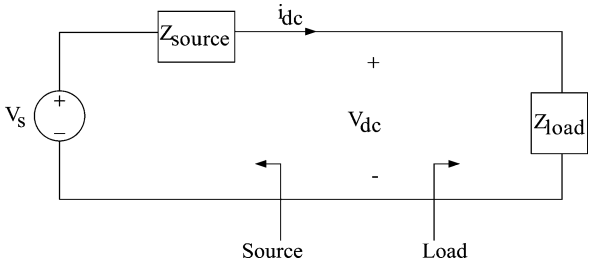

Fig. 11. System representation of a simplified dc power system.

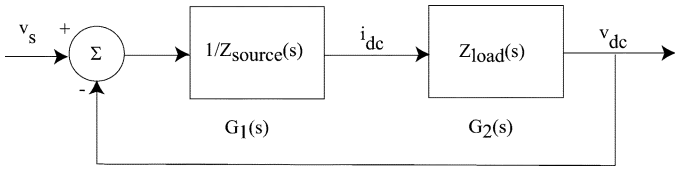

Fig. 12. Continuous control representation of the system.

VII. Consideration of System Small-Signal Stability

The stability of power-electronics-based distribution systems is a significant design consideration due to the high-bandwidth control offered by modern computers and power handling components. One technique that is often applied to investigate the stability of dc power-electronics-based systems is the method of generalized impedance analysis. To apply this method, a system is partitioned (or grouped) into a generalized source and load as shown in Fig. 11. The small-signal impedance characteristics of the source (denoted Z_{source}) and the load (denoted Z_{load}) obtained at an operating point of interest are used to determine the local behavior and stability of the system. A block diagram representing the closed-loop source/load system is shown in Fig. 12.

The system interaction is modeled in the frequency domain, wherein the transfer function between source and load is represented as

$$\frac{v_{dc}(s)}{v_s(s)} = \frac{1}{1 + \frac{Z_{\text{source}}(s)}{Z_{\text{load}}(s)}}. \tag{18}$$

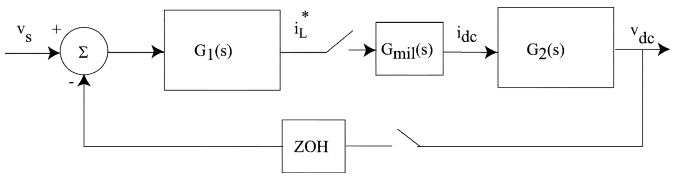

Fig. 13. Discrete control representation of the system.

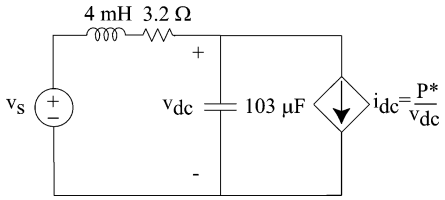

Fig. 14. Example source with constant power load.

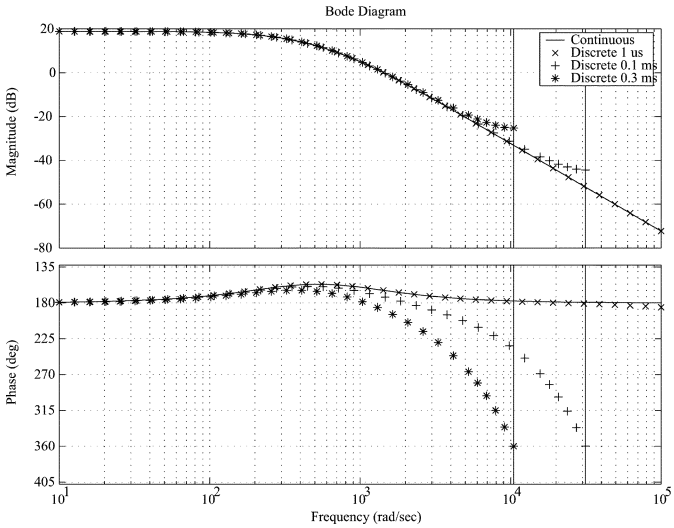

Fig. 15. Bode diagrams of a system in continuous and discrete sense.

Using the Nyquist criteria, one maps the contour of $Z_{\text{load}}/Z_{\text{source}}$ to ensure that it does not encircle -1. This guarantees that the considered operating point is stable. A number of stability criterion have been proposed based upon this generalized technique [19]–[21].

MIL is a useful tool for investigating system stability. One of the primary benefits is the capability to investigate a wide range of source parameters prior to construction. However, it is important to note that the capability of MIL to represent the physical all-hardware system is a function of the sampling rate between simulation and hardware. As the sampling frequency is decreased, the stability of overall system is decreased. To show this, the dynamics of a MIL system are represented in block diagram form in Fig. 13. From this diagram, it can be shown that the output voltage of the MIL-based system can be expressed in terms of source voltage in the Z-domain as

$$v_{dc}(z) = \frac{G_2(z)(G_1 v_s(z))}{1 + G_1(z)G_2(z)} \tag{19}$$

where

$$G_1(z) = \mathcal{Z}(G_1(s)H_{zoh}(s)) \tag{20}$$

$$G_2(z) = \mathcal{Z}(G_2(s)G_{mil}(s)). \tag{21}$$

The open-loop transfer function of the system shown in Fig. 13 is

$$G(z) = G_1(z)G_2(z). \tag{22}$$

Equation (18) represents the dynamics of the system in which all components are implemented in hardware. In contrast, (19) represents the dynamics when MIL is introduced. The capability of (19) to represent (18) for stability analysis is dependent upon the sampling frequency. To illustrate differences caused by sampling and its influence on system stability, the system shown in Fig. 14 was implemented using Matlab. In this system, the source impedance is a series resistor/inductor with values of 3.22 Ω and 4 mH. The load is a capacitor in parallel with a converter working as a constant-power-load (CPL), that has a command voltage and power values of 150 V and 800 W, respectively. The values of series resistance, inductance, and bus capacitance were selected based upon values of filter components used in the dc testbed. The 800-W power level (low relative to a 3.7-kW rating of the generator) was chosen so that the system was certain to be stable in the steady-state. This provided a means to ensure that respective instabilities were indeed the result of low sampling, and not source/load interactions. The bode diagram of this dc system represented using both continuous and discrete analysis is shown in Fig. 15. It can be seen that a system that is stable in continuous time, is predicted to be unstable as the sampling frequency of MIL is reduced. Specifically, at the sampling rate of 1 μs, the MIL and continuous system results are nearly identical; however, when the sampling period is increased to 0.3 ms, the phase margin becomes negative, which would predict an unstable system. Similar observations have been reported in [22] wherein several methods of selecting the sampling rate to ensure stability of a continuous plant with sampled controllers are also discussed.

VIII. Conclusion

An MIL infrastructure has been set forth and applied to a zonal dc distribution system being considered for future naval applications. An effective system partitioning and interface of models/hardware at the power level has been demonstrated. An example synchronous machine/rectifier power source was used to validate the approach in both time and frequency domains. It was shown that the measured large-displacement time-domain responses and small-displacement frequency-domain characteristics (impedances) for the detailed simulation and MIL implementations are in close agreement, which validates the proposed approach as an effective tool for system-level design and analysis. The use of MIL for system-level stability analysis has been also been considered and is shown to be dependent upon the sampling frequency of the model/hardware interface.

REFERENCES

[1] P. Terwiesch, T. Keller, and E. Scheiben, "Rail vehicle control system integration testing using digital hardware-in-the-loop simulation," *IEEE Trans. Control Syst. Technol.*, vol. 7, no. 3, pp. 352–362, May 1999.

[2] S. Abourida, C. Dufour, J. Belanger, G. Murere, N. lechevin, and B. Yu, "Real-time PC based simulator of electric systems and drives," in *Proc. 17th IEEE Applied Power Electronics Conf. Expo*, Mar. 10–14, 2002, pp. 433–438.

[3] J. C. Lee and M. W. Suh, "Hardware-in-the-loop simulator for ABS/TCS," in *Proc. 1999 IEEE Int. Conf. Control Applications*, Aug. 22–27, 1999, pp. 652–657.

[4] A. Monti, E. Santi, R. Dougal, and M. Riva, "Rapid prototyping of digital controls for power electronics," *IEEE Trans. Power Electron.*, vol. 18, no. 3, pp. 915–923, May 2003.

[5] V. R. Dinavahi, M. R. Iravani, and R. Bonert, "Real-time digital simulation of power electronic apparatus interfaced with digital controllers," *IEEE Trans. Power Delivery*, vol. 16, no. 4, pp. 775–781, Oct. 2001.

[6] H. Slater, D. Atkinson, and A. Jack, "Real-time emulation for power equipment develoment. Part 2: The virtual machine," *Proc. Inst. Elect. Eng.*, vol. 145, no. 3, pp. 153–158, May 1998.

[7] H. Taoka, I. Iyoda, H. Noguchi, N. Sato, Nakazawa, and T. Yamazaki, "A real-time digital simulator with digital/analog conversion interface for testing power instruments," *IEEE Trans. Power Syst.*, vol. 9, no. 2, pp. 862–868, May 1994.

[8] S. Ayasun, S. Vallieu, R. Fishl, and T. Chmielewski, "Electric machinery diagnostic/testing system and power hardware-in-the-loop studies," in *Proc. 4th IEEE Int. Symp. Diagnostics Electric Machines, Power Electronics Drives*, Atlanta, GA, Aug. 24–26, 2003, pp. 361–366.

[9] S. D. Pekarek *et al.*, "Development of a testbed for design and evaluation of power electronic based generation and distribution system," in *Proc. SAE'02 Power Systems Conf.*, Coral Springs, FL, Oct. 29–31, 2002.

[10] "Simulink: Dynamic system simulation for Matlab," in *Using Simulink Version 3*. Natick, MA: The MathWorks Inc., 1999.

[11] O. Wasynczuk and S. D. Sudhoff, "Automated state model generation algorithm for power circuits and systems," *IEEE Trans. Power Syst.*, vol. 11, no. 4, pp. 1951–1956, Nov. 1996.

[12] *User's Manual of Real Time Toolbox*, HUMUSOFT, Prague, Czech Republic, 2001.

[13] E. Walters, O. Wasynczuk, J. Jatskevich, and E. Lucas, "An observer-based automated averaging technique for power electronic circuits," in *Proc. SAE Power Systems Conf.*, San Diego, CA, Oct. 2000, pp. 101–108.

[14] J. T. Tou, *Digital and Sampled-Data Control Systems*. New York: McGraw-Hill, 1959.

[15] S. D. Pekarek, O. Wasynczuk, and H. J. Hegner, "An efficient and accurate model for the simulation and analysis of synchronous machine/converter systems," *IEEE Trans. Energy Conv.*, vol. 13, no. 1, pp. 42–48, Mar. 1998.

[16] S. D. Pekarek *et al.*, "An efficient multi-rate simulation technique for power-electronic-based systems," *IEEE Trans. Power Syst.*, vol. 19, no. 1, pp. 399–409, Feb. 2004.

[17] W. Gautchi, *Numerical Analysis: An Introduction*. Boston, MA: Birkhauser, 1997.

[18] S. D. Sudhoff, K. A. Corzine, H. J. Hegner, and D. E. Delisle, "Transient and dynamic average-value modeling of synchronous machine fed load-commutated converters," *IEEE Trans. Energy Conv.*, vol. 11, no. 3, pp. 508–514, Sep. 1996.

[19] S. D. Sudhoff, S. F. Glover, P. T. Lamm, D. H. Schmucker, and D. E. Delisle, "Admittance space stability analysis of power electronic systems," *IEEE Trans. Aerosp. Electron. Syst.*, vol. 36, pp. 965–973, Jul. 2000.

[20] C. Wildrick, F. C. Lee, B. Cho, and B. Choi, "A method of defining the load impedance specification for a stable distributed power system," *IEEE Trans. Power Electron.*, vol. 10, no. 3, pp. 280–285, May 1995.

[21] X. Feng, J. Liu, and F. C. Lee, "Impedance specifications for stable dc distributed power systems," *IEEE Trans. Power Electron.*, vol. 17, no. 2, pp. 157–162, Mar. 2002.

[22] S. P. Chicatelli and T. T. Hartley, "A criterion for guaranteed closed loop simulation stability," in *Proc. 34th Midwest Symp. Circuits Systems*, vol. 1, May 1991, pp. 509–512.

Weidong Zhu received the B.S. and M.S. degrees in electrical engineering from Shanghai Jiao-tong University, Shanghai, China, in 1995 and 1998, respectively, and is currently pursuing the Ph.D degree in electrical engineering at the University of Missouri-Rolla.

From 1998 to 2001, he was an Electrical Engineer for the Shanghai Engineering Center, ABB China, Shanghai. His interests include analysis and design of power electronics-based electromechanical systems.

Steve Pekarek (S'89–M'96) received the Ph.D. degree in electrical engineering from Purdue University, West Lafayette, IN, in 1996.

From 1997 to 2004, he was an Assistant (Associate) Professor of electrical and computer engineering at the University of Missouri-Rolla (UMR). He is presently an Associate Professor of electrical and computer engineering at Purdue University and is a co-Director of the Energy Systems Analysis Consortium. As a faculty member he has been the principal investigator on a number of successful research programs including projects for the Navy, Air Force, Ford Motor Company, Motorola, and Delphi Automotive Systems. The primary focus of these investigations has been the analysis and design of power electronic based architectures for finite inertia power and propulsion systems.

Juri Jatskevich (M'99) received the B.S.E.E. degree from UNAU, Kiev, Ukraine, in 1994, and the M.S.E.E. and the Ph.D. degrees from Purdue University, West Lafayette, IN, in 1997 and 1999, respectively.

He is presently an Assistant Professor of electrical and computer engineering at the University of British Columbia, Vancouver, BC, Canada. His research interests include electrical machines, power electronic systems, and simulation.

Oleg Wasynczuk (M'76–SM'88) was born in Chicago, IL, on June 26, 1954. He received the B.S.E.E. degree from Bradley University, Peoria, IL, in 1976, and the M.S.E.E. and Ph.D. degrees from Purdue University, West Lafayette, IN, in 1977 and 1979, respectively.

Currently, he is a Professor in the School of Electrical and Computer Engineering, Purdue University. He has authored or co-authored over 60 technical papers and has co-authored *Analysis of Electric Machinery* (Piscataway, NJ: IEEE Press) and *Electromechanical Motion Devices* (New York: McGraw-Hill). His areas of interest are power system dynamics and control and the analysis and design of electromechanical devices.

Dr. Wasynczuk is currently the Vice Chair of the Synchronous Machinery Subcommittee of the IEEE.

Dana E. Delisle received the B.S.E.E. from the University of Massachusetts, Boston, in 1984.

He is employed with the Electrical System Division, Naval Sea Systems Command, Washington, DC. For the past decade, he has specialized in dc electric power systems for Navy shipboard electronic systems.